FRIEDRICH-ALEXANDER-UNIVERSITÄT ERLANGEN-NÜRNBERG
INSTITUT FÜR INFORMATIK (MATHEMATISCHE MASCHINEN UND DATENVERARBEITUNG)

Lehrstuhl für Informatik 10 (Systemsimulation)

Resolving Ill-posedness of Rigid Multibody Dynamics

T. Preclik, U. Rüde, C. Popa

Technical Report 10-11

Resolving Ill-posedness of Rigid Multibody Dynamics

T. Preclik*, U. Rüde†, C. Popa‡

4th March 2011

Abstract

Rigid multibody dynamics are often subject to redundant constraints. In the context of contacts it is usually not clear which constraints can be removed in order to obtain a correct solution. But also in the context of jointed multibody systems the removal of redundant constraints selects a particular solution of the underdetermined problem. In case of dissipative systems this also affects the velocity solution and thus the evolution of the dynamic system. In this report this problem is demonstrated exemplarily by means of a table sliding down a ramp. An alternative approach is suggested, which keeps redundant constraints but regularizes the ill-posed problem in a physically motivated way such that a unique solution is obtained.

1 Introduction

Rigid bodies move in accordance with Newton's second law of motion, which is an ordinary differential equation (ODE). When the bodies' motions become restricted, for example by attaching bilateral joints between them, algebraic equations, which describe the motion constraints, are added to the differential equations. Thus the system is no longer composed of ODEs but of differential algebraic equations (DAEs). In the simplest case the joint completely constrains the relative motion at a common point of the bodies. Then the gap between the two involved points must vanish at all times:

$$\boldsymbol{g}(\boldsymbol{q}(t), \boldsymbol{\varphi}(t)) = 0, \tag{1}$$

where $\boldsymbol{q}(t)$ are the positions and $\boldsymbol{\varphi}(t)$ are the orientations. At the joint location then a joint reaction force $\boldsymbol{\lambda} \in \mathbb{R}^3$ is present, which is not allowed to do work.

When bodies come into contact, the unilateral contact constraint can no longer be described by an equation but must be described in terms of a complementarity condition. The gap in normal direction must then be non-negative ($g_{i_n}(\boldsymbol{q}(t), \boldsymbol{\varphi}(t)) \geq 0$) to prevent penetration of the bodies, but may certainly break contact. Contact reaction forces in normal direction are acting at the contact and must be repulsive but not adhesive ($\lambda_{i_n} \geq 0$). Also the reaction force may only act if and only if the bodies are actually in contact ($\lambda_{i_n} \cdot g_{i_n}(\boldsymbol{q}(t), \boldsymbol{\varphi}(t)) = 0$). These conditions together form the complementarity condition, which can be written down in a compact notation:

$$g_{i_n}(\boldsymbol{q}(t), \boldsymbol{\varphi}(t)) \geq 0 \perp \lambda_{i_n} \geq 0 \tag{2}$$

*University of Erlangen-Nürnberg, Computer Science 10, System Simulation, tobias.preclik@informatik.uni-erlangen.de
†University of Erlangen-Nürnberg, Computer Science 10, System Simulation, ulrich.ruede@informatik.uni-erlangen.de
‡Ovidius University of Constanta, Faculty of Mathematics and Informatics, cpopa@univ-ovidius.ro

Adding complementarity constraints to the system prevents us from formulating a system of DAEs but requires us to formulate differential complementarity problems (DCPs) or in a more general setting differential variational inequalities (DVIs).

Eq. 2 has one little catch: A force can never instantaneously produce a velocity jump. The latter is necessary e.g. for impacts. Consider the example of a ball (inelastically) impacting the ground. At the time of impact the ball abruptly comes to rest, that is the velocity jumps to zero. Thus the linear and angular velocities $\boldsymbol{u}(t) = (\boldsymbol{v}(t)^T, \boldsymbol{\omega}(t)^T)^T$ are assumed to be of locally bounded variation such that $\boldsymbol{u}(t)$ may have discontinuities. However, for every time instant left- and right-limits $\boldsymbol{u}^-(t)$ and $\boldsymbol{u}^+(t)$ exist, which are equivalent to the respective one-sided derivatives. Thus $(\boldsymbol{q}(t)^T, \boldsymbol{\varphi}(t)^T)^T$ is no longer assumed to be differentiable everywhere, but it is still the time integral of the velocity function $\boldsymbol{u}$. Since accelerations cannot be expected to exist everywhere, one instead considers a differential measure. Similarly contact forces are replaced by contact impulsions. However for the remainder of this document we set that distinction aside from conviction that the considerations still hold. A more thorough investigation will be part of future work.

Naturally the system of rigid bodies is restricted not only by one constraint between a single pair of bodies, but an arbitrary number of constraints can be present. The constraint index $i \in \{1, \dots, n_c\}$ will be used from now on as a subscript to distinguish n_c constraints:

$$\boldsymbol{g_i}(\boldsymbol{q}(t), \boldsymbol{\varphi}(t)) = \boldsymbol{0},\ \boldsymbol{\lambda_i} \in \mathbb{R}^3 \tag{3a}$$

$$g_{i_n}(\boldsymbol{q}(t), \boldsymbol{\varphi}(t)) \geq 0 \perp \lambda_{i_n} \geq 0 \tag{3b}$$

When introducing multiple constraints, it becomes also clear that we can *over-constrain* a system, that is add more constraints than necessary to achieve a restricted motion. As an example consider a table on the ground. All four legs are either nailed down or touch the ground. In order to prevent the table from penetrating the ground, reaction forces must act at each leg i. Different solutions exist satisfying the constraints. The normal reaction forces located diagonally across must be of the same magnitude to prevent rotation and the total sum must be mg where g is the gravitational acceleration and m is the mass of the table. In fact only two of the constraints are necessary to keep the table from penetrating the ground. Thus when solving for reaction impulses we are faced with a problem whose solution is underdetermined. This can negatively influence the reliability and convergence of the solving method employed. But if we obtain a solution the question remains, whether it is reasonable or not. In this particular case the velocities and positions obtained when applying the reaction are still unique. Hence we might be willing to ignore the underdeterminacy under these circumstances. However, even here we may not base any critical calculations on the computed reactions.

The model as it currently stands lacks friction. An accepted model for dry frictional contacts is the Coulomb friction law. It states that the magnitude of the friction force is less or equal to the normal reaction force times a coefficient of friction ($\|\boldsymbol{\lambda}_{\boldsymbol{i}_{t,o}}\|_2 \leq \mu_i \lambda_{i_n}$). Furthermore, in the case where the friction force is not able to keep the contact point in place, that is the friction force is at its limit ($\|\boldsymbol{\lambda}_{\boldsymbol{i}_{t,o}}\|_2 = \mu_i \lambda_{i_n}$), the friction force must do its utmost to prevent sliding, which is the case when it directly opposes slip ($\boldsymbol{\lambda}_{\boldsymbol{i}_{t,o}} = -\mu_i \lambda_{i_n} \frac{\dot{\boldsymbol{g}}_{\boldsymbol{i}_{t,o}}(\boldsymbol{q}(t), \boldsymbol{\varphi}(t))}{\|\dot{\boldsymbol{g}}_{\boldsymbol{i}_{t,o}}(\boldsymbol{q}(t), \boldsymbol{\varphi}(t))\|_2}$). In 2D these conditions can be expressed in terms of a complementarity condition if the normal reaction λ_{i_n} is known to be $\bar{\lambda}_{i_n}$ in advance:

$$g_{i_t}(\boldsymbol{q}(t), \boldsymbol{\varphi}(t)) \gtreqless 0 \perp -\mu_i \bar{\lambda}_{i_n} \leq \lambda_{i_t} \leq \mu_i \bar{\lambda}_{i_n} \tag{4}$$

This complementarity condition includes arbitrary upper as well as lower bounds. It states that the left-hand side must vanish if the unknown is within its bounds. If the unknown is bounded above, the left-hand side must be less or equal to 0 and if it is bounded below, the left-hand side must be greater or equal to 0. Suffice it to

say that such box-constrained complementarity conditions can be equivalently stated in terms of three standard complementarity conditions.

In three-dimensional space we can formulate the law in terms of a two-dimensional variational inequality or a two-dimensional complementarity problem

$$\boldsymbol{\lambda}_{\boldsymbol{i}_{t,o}} \in \mathcal{S}(\mu_i(t)\bar{\lambda}_{i_n}), \quad g_{\boldsymbol{i}_{t,o}}(\boldsymbol{q}(t), \boldsymbol{\varphi}(t))^T(\boldsymbol{x} - \boldsymbol{\lambda}_{\boldsymbol{i}_{t,o}}) \geq 0, \quad \forall \boldsymbol{x} \in \mathcal{S}(\mu_i(t)\bar{\lambda}_{i_n}) \tag{5a}$$

$$\boldsymbol{g}_{\boldsymbol{i}_{t,o}}(\boldsymbol{q}(t), \boldsymbol{\varphi}(t)) \in \mathcal{N}_{\mathcal{S}(\mu_i(t)\bar{\lambda}_{i_n})}(\boldsymbol{\lambda}_{\boldsymbol{i}_{t,o}}) \perp \boldsymbol{\lambda}_{\boldsymbol{i}_{t,o}} \in \mathcal{S}(\mu_i(t)\bar{\lambda}_{i_n}) \tag{5b}$$

where $\mathcal{S}(r)$ is the disc with radius r ($\mathcal{S}(r) = \{\boldsymbol{x} \in \mathbb{R}^2 \mid \|\boldsymbol{x}\|_2 \leq r\}$) and $\mathcal{N}_{\mathcal{K}}(\boldsymbol{x})$ is the normal cone of $\mathcal{K}$ at $\boldsymbol{x}$ ($\mathcal{N}_{\mathcal{K}}(\boldsymbol{x}) = \{\boldsymbol{y} \mid \boldsymbol{y}^T(\boldsymbol{x} - \boldsymbol{x}^*) \geq 0, \forall \boldsymbol{x}^* \in \mathcal{K}\}$). Regardless of whether we use the exact formulation or an approximation or fall back to the box-constrained complementarity condition, there is one caveat. The limits always depend on the normal reaction, which is a priori unknown. In the case of the table this means that the friction limits depend on the precise normal reactions. This in turn implies that possibly more or less energy can be dissipated at the contacts if the coefficients of friction are different. Consequently, solutions exist differing in their energy and thus velocities and positions. This tells us that the problem is ill-posed and cannot properly capture the physics.

2 Constraint-based Formulation

In the following we try to illustrate the ill-posedness by means of a frictional table sliding on the floor. Therefore the problem is formulated by constraining the equations of motions, which results in a system of differential algebraic equations (DAE), which will be discretized by a semi-implicit time-integration. We deliberately refrain from formulating complementarity constraints since they are not relevant for the discussion and would render it unnecessarily cumbersome. Instead we assume that the contacts persist and that the contacts are exclusively dynamic.

2.1 Equations of Motion

The table is assumed to be rigid and as such it can be described by the state variables $\boldsymbol{q}$, $\boldsymbol{\varphi}$, $\boldsymbol{v}$ and $\boldsymbol{\omega}$, where $\boldsymbol{q} \in \mathbb{R}^3$ is the center of gravity of the table, $\boldsymbol{\varphi} \in \mathrm{SO}(3)$ is a description of the orientation of the table. $\mathrm{SO}(3)$ denotes the special orthogonal group in $\mathbb{R}^3$ representing all possible proper rotations. In the following we will use quaternions to represent the bodies' orientation. $\boldsymbol{v}(t) : \mathbb{R} \to \mathbb{R}^3$ and $\boldsymbol{\omega}(t) : \mathbb{R} \to \mathbb{R}^3$ are the linear and angular velocity respectively. The change in time of position can be easily expressed in terms of the velocity:

$$\dot{\boldsymbol{q}}(t) = \boldsymbol{v}(t) \tag{6}$$

However, the change of orientation in time depends on the orientation in turn. In case of quaternions the differential equation for one body $j \in \{1, \ldots, n_b\}$ out of n_b bodies in total reads

$$\dot{\boldsymbol{\varphi}}_j(t) = \frac{1}{2}(0, \boldsymbol{\omega}_j(t)) \cdot \boldsymbol{\varphi}_j(t), \tag{7}$$

where the operator "$\cdot$" denotes the quaternion product here and (x_0, x_1, x_2, x_3) represents the quaternion $x_0 + x_1 \cdot \mathrm{i} + x_2 \cdot \mathrm{j} + x_3 \cdot \mathrm{k}$ with scalar component x_0. The quaternion product can be rewritten in terms of a matrix product:

$$\dot{\boldsymbol{\varphi}}_j(t) = \frac{1}{2}\begin{bmatrix} -\varphi_{j_1}(t) & -\varphi_{j_2}(t) & -\varphi_{j_3}(t) \\ \varphi_{j_0}(t) & \varphi_{j_3}(t) & -\varphi_{j_2}(t) \\ -\varphi_{j_3}(t) & \varphi_{j_0}(t) & \varphi_{j_1}(t) \\ \varphi_{j_2}(t) & -\varphi_{j_1}(t) & \varphi_{j_0}(t) \end{bmatrix} \boldsymbol{\omega}_j(t) = \mathbf{Q}(\boldsymbol{\varphi}_j(t))\boldsymbol{\omega}_j(t) \tag{8}$$

Let $\mathbf{Q}(\boldsymbol{\varphi}(t))$ denote the block diagonal matrix of all $\mathbf{Q}(\boldsymbol{\varphi}_j(t))$. Combining Eq. (6) and Eq. (8) results in

$$\begin{pmatrix} \dot{\boldsymbol{q}}(t) \\ \dot{\boldsymbol{\varphi}}(t) \end{pmatrix} = \begin{bmatrix} \mathbf{I} & \\ & \mathbf{Q}(\boldsymbol{\varphi}(t)) \end{bmatrix} \begin{pmatrix} \boldsymbol{v}(t) \\ \boldsymbol{\omega}(t) \end{pmatrix}. \tag{9}$$

Newton's second law of motion for the linear momentum and the momentum conservation laws in general state that the net force and torque is equal to the rate of change of momentum:

$$\begin{aligned} \dot{\boldsymbol{p}}_j(t) &= \frac{\mathrm{d}(m_j\boldsymbol{v}_j(t))}{\mathrm{d}t} = \dot{m}_j\boldsymbol{v}_j(t) + m_j\dot{\boldsymbol{v}}_j(t) = m_j\dot{\boldsymbol{v}}_j(t) = \mathrm{diag}(m_j, m_j, m_j)\dot{\boldsymbol{v}}_j(t) = \hat{\mathbf{M}}_j\dot{\boldsymbol{v}}_j(t) = \boldsymbol{f}_j(t) \\ \dot{\boldsymbol{L}}_j(t) &= \frac{\mathrm{d}(\boldsymbol{\Theta}_j(t)\boldsymbol{\omega}_j(t))}{\mathrm{d}t} = \boldsymbol{\Theta}_j(t)\dot{\omega}_j(t) + \dot{\boldsymbol{\Theta}}_j(t)\omega_j(t) = \boldsymbol{\Theta}_j(t)\dot{\boldsymbol{\omega}}_j(t) - (\boldsymbol{\Theta}_j(t)\boldsymbol{\omega}_j(t)) \times \boldsymbol{\omega}_j(t) = \boldsymbol{\tau}_j(t) \end{aligned} \tag{10}$$

Combining Eq. (9) and Eq. (10) leads to the (nonlinear) ordinary differential equations (ODE)

$$\begin{aligned} \begin{pmatrix} \dot{\boldsymbol{q}}(t) \\ \dot{\boldsymbol{\varphi}}(t) \end{pmatrix} &= \begin{pmatrix} \boldsymbol{v}(t) \\ \mathbf{Q}(\boldsymbol{\varphi}(t))\boldsymbol{\omega}(t) \end{pmatrix} \\ \begin{bmatrix} \hat{\mathbf{M}} & \\ & \boldsymbol{\Theta}(t) \end{bmatrix} \begin{pmatrix} \dot{\boldsymbol{v}}(t) \\ \dot{\boldsymbol{\omega}}(t) \end{pmatrix} = \mathbf{M}(t) \begin{pmatrix} \dot{\boldsymbol{v}}(t) \\ \dot{\boldsymbol{\omega}}(t) \end{pmatrix} &= \begin{pmatrix} \boldsymbol{f}(t) \\ \boldsymbol{\tau}(t) - \boldsymbol{\omega}(t) \times \boldsymbol{\Theta}(t)\boldsymbol{\omega}(t) \end{pmatrix}, \end{aligned} \tag{11}$$

where $\hat{\mathbf{M}}$ is the collection of all $\hat{\mathbf{M}}_j$ in a block diagonal matrix, $\mathbf{M}(t)$ is the mass matrix and $\boldsymbol{\Theta}$ is the collection of all $\boldsymbol{\Theta}_j$ in a block diagonal matrix. $\boldsymbol{f}$ and $\boldsymbol{\tau}$ are the collections of $\boldsymbol{f}_j$ and $\boldsymbol{\tau}_j$ in a column vector respectively. The cross product is generalized to a multiple of three components as follows. The cross product of a vector $\boldsymbol{a} = (a_1, a_2, a_3)^T \in \mathbb{R}^3$ with another vector $\boldsymbol{b} \in \mathbb{R}^3$ can be expressed in terms of a 3×3 anti-symmetric matrix $\mathbf{a}^\times$:

$$\boldsymbol{a} \times \boldsymbol{b} = \begin{bmatrix} 0 & -a_3 & a_2 \\ a_3 & 0 & -a_1 \\ -a_2 & a_1 & 0 \end{bmatrix} \boldsymbol{b} = \mathbf{a}^\times \boldsymbol{b} \tag{12}$$

A cross product between vectors representing a collection of three-dimensional vectors can then be expressed by collecting the anti-symmetric matrices corresponding to the subvectors of the left operand in a block diagonal matrix and performing a matrix-vector multiplication instead.

2.2 Constraints

Fig. 1 illustrates the setup. The table initially rests on a plane with the normal vector $\boldsymbol{n} = (0, 0, 1)^T$. Since we assume that the table will slide on the plane in the course of the simulation, we pose constraints on the positions of the legs. The position of the i-th contact on the plane at time t is

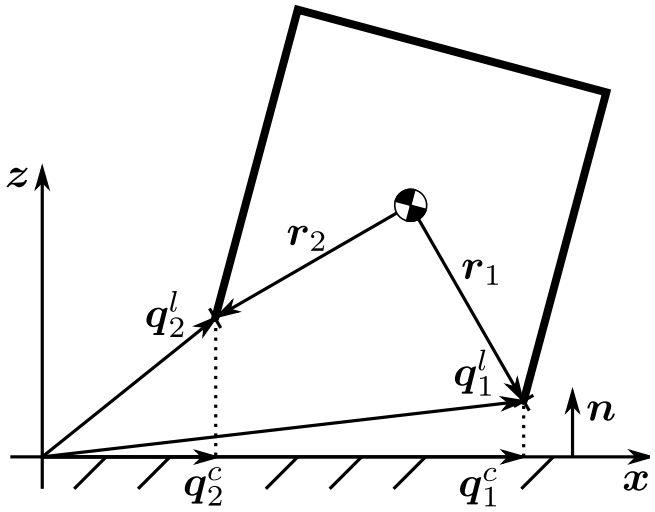

Figure 1: Sketch of the table setup.

$$\boldsymbol{q}_i^c(\boldsymbol{q}(t),\boldsymbol{\varphi}(t)) = \boldsymbol{q}_i^l(\boldsymbol{q}(t),\boldsymbol{\varphi}(t)) - \boldsymbol{n}^T(\boldsymbol{q}_i^l(\boldsymbol{q}(t),\boldsymbol{\varphi}(t)) - \boldsymbol{a}) \cdot \boldsymbol{n}, \tag{13}$$

where $\boldsymbol{a}$ is a point in the plane and $\boldsymbol{q}_i^l(t)$ is the position of the i-th leg in the world frame. The legs' positions can be stated in terms of the position of the center of gravity and the rotation of the initial configuration:

$$\boldsymbol{q}_i^l(\boldsymbol{q}(t),\boldsymbol{\varphi}(t)) = \boldsymbol{q}(t) + \boldsymbol{\varphi}(t) \cdot \boldsymbol{r}_i^0 \cdot \overline{\boldsymbol{\varphi}(t)} = \boldsymbol{q}(t) + \boldsymbol{r}_i(\boldsymbol{\varphi}(t)) \tag{14}$$

Here the operator "$\cdot$" again represents the quaternion product, $\boldsymbol{r}_i^0$ is the vector pointing from the center of gravity of the body to the i-th leg in the unrotated body frame. $\overline{\boldsymbol{\varphi}(t)}$ is the conjugate quaternion of $\boldsymbol{\varphi}(t)$. Note that there is just a single body involved such that $\boldsymbol{q} \in \mathbb{R}^3$, $\boldsymbol{\varphi} \in \mathbb{R}^4$ and $n_b = 1$.

The relative position is $\boldsymbol{q}_i^l(t) - \boldsymbol{q}_i^c(t)$ and can be expressed in terms of the (orthonormal) contact frames $\boldsymbol{n}_i = \boldsymbol{n}$, $\boldsymbol{t}_i = \boldsymbol{t} = (1,0,0)^T$ and $\boldsymbol{o}_i = \boldsymbol{o} = (0,1,0)^T$ by multiplying the relative position with $[\boldsymbol{n},\boldsymbol{t},\boldsymbol{o}]^T$ from the left. The contact frames are assumed to be identical for all contacts here. For the next step we will pretend to deal with a bilateral ball joint instead of a frictional unilateral contact on the grounds that a frictional contact very much behaves like a joint. The only difference is that the contact reaction forces are constrained and cannot unconditionally hold the table in place. For the bilateral joint the constraint states that the relative position must be zero:

$$\boldsymbol{g}_i(\boldsymbol{q}(t),\boldsymbol{\varphi}(t)) = [\boldsymbol{n},\boldsymbol{t},\boldsymbol{o}]^T \left(\boldsymbol{q}_i^l(\boldsymbol{q}(t),\boldsymbol{\varphi}(t)) - \boldsymbol{q}_i^c(\boldsymbol{q}(t),\boldsymbol{\varphi}(t))\right) = \boldsymbol{0} \tag{15}$$

The collection of all $\boldsymbol{g}_i$ in a vector is called $\boldsymbol{g}$. Since $\boldsymbol{g}$ does not depend on the velocities it is called a holonomic constraint. Differentiating $\boldsymbol{g}$ w.r.t. time leads to

$$\dot{\boldsymbol{g}}(\boldsymbol{q}(t),\boldsymbol{\varphi}(t)) = \mathbf{J}_{\boldsymbol{g}}(\boldsymbol{q}(t),\boldsymbol{\varphi}(t)) \begin{bmatrix} \mathbf{I} & \\ & \mathbf{Q}(\boldsymbol{\varphi}(t)) \end{bmatrix} \begin{pmatrix} \boldsymbol{v}(t) \\ \boldsymbol{\omega}(t) \end{pmatrix} = \mathbf{J}(\boldsymbol{q}(t),\boldsymbol{\varphi}(t)) \begin{pmatrix} \boldsymbol{v}(t) \\ \boldsymbol{\omega}(t) \end{pmatrix}. \tag{16}$$

Adding the constraints of Eq. (15) and Lagrange multipliers $\boldsymbol{\lambda}$ to the ODE in Eq. (11) results in a system of differential algebraic equations (DAE)

$$\begin{pmatrix} \dot{\boldsymbol{q}}(t) \\ \dot{\boldsymbol{\varphi}}(t) \end{pmatrix} = \begin{pmatrix} \boldsymbol{v}(t) \\ \mathbf{Q}(\boldsymbol{\varphi}(t))\boldsymbol{\omega}(t) \end{pmatrix} \tag{17a}$$

$$\mathbf{M}(t) \begin{pmatrix} \dot{\boldsymbol{v}}(t) \\ \dot{\boldsymbol{\omega}}(t) \end{pmatrix} = \begin{pmatrix} \boldsymbol{f}(t) \\ \boldsymbol{\tau}(t) - \boldsymbol{\omega}(t) \times \boldsymbol{\Theta}(t)\boldsymbol{\omega}(t) \end{pmatrix} + \mathbf{J}(\boldsymbol{q}(t), \boldsymbol{\varphi}(t))^T \boldsymbol{\lambda} \tag{17b}$$

$$\boldsymbol{g}(\boldsymbol{q}(t), \boldsymbol{\varphi}(t)) = \mathbf{0} \tag{17c}$$

where $n_c = 4$ and $\lambda = (\lambda_{1_n}, \lambda_{1_t}, \lambda_{1_o}, \ldots, \lambda_{4_n}, \lambda_{4_t}, \lambda_{4_o})^T$.

2.3 Time Discretization

Eq. (17) can be conveniently discretized using a semi-implicit Euler discretization, meaning that velocities are integrated first and then the new velocities are used to integrate positions implicitly. The algebraic equation (17c) should be satisfied in the next time step. This leads to the following time-discrete linear system of equations (LSE) for one time step δt, where a prime sign $'$ indicates variables at time $t + \delta t$ in contrast to variables at time t without a prime sign:

$$\begin{pmatrix} \tilde{\boldsymbol{q}}' \\ \tilde{\boldsymbol{\varphi}}' \end{pmatrix} = \delta t \begin{pmatrix} \tilde{\boldsymbol{v}}' \\ \mathbf{Q}(\tilde{\boldsymbol{\varphi}})\tilde{\boldsymbol{\omega}}' \end{pmatrix} + \begin{pmatrix} \tilde{\boldsymbol{q}} \\ \tilde{\boldsymbol{\varphi}} \end{pmatrix} \tag{18a}$$

$$\begin{pmatrix} \tilde{\boldsymbol{v}}' \\ \tilde{\boldsymbol{\omega}}' \end{pmatrix} = \delta t \tilde{\mathbf{M}}^{-1} \begin{pmatrix} \tilde{\boldsymbol{f}} \\ \tilde{\boldsymbol{\tau}} - \tilde{\boldsymbol{\omega}} \times \tilde{\boldsymbol{\Theta}}\tilde{\boldsymbol{\omega}} \end{pmatrix} + \delta t \tilde{\mathbf{M}}^{-1} \mathbf{J}(\tilde{\boldsymbol{q}}, \tilde{\boldsymbol{\varphi}})^T \tilde{\boldsymbol{\lambda}} + \begin{pmatrix} \tilde{\boldsymbol{v}} \\ \tilde{\boldsymbol{\omega}} \end{pmatrix} \tag{18b}$$

$$\boldsymbol{g}(\tilde{\boldsymbol{q}}', \tilde{\boldsymbol{\varphi}}') = \boldsymbol{g}(\tilde{\boldsymbol{q}}, \tilde{\boldsymbol{\varphi}}) + \delta t \dot{\boldsymbol{g}}(\tilde{\boldsymbol{q}}, \tilde{\boldsymbol{\varphi}}) = \boldsymbol{g}(\tilde{\boldsymbol{q}}, \tilde{\boldsymbol{\varphi}}) + \delta t \mathbf{J}(\tilde{\boldsymbol{q}}, \tilde{\boldsymbol{\varphi}}) \begin{pmatrix} \tilde{\boldsymbol{v}}' \\ \tilde{\boldsymbol{\omega}}' \end{pmatrix} = \mathbf{0} \tag{18c}$$

If indeed the table were fixed to the plane by joints, we would be done. To solve Eq. (18), we insert (18b) into (18c) and solve for the Lagrange multipliers $\tilde{\boldsymbol{\lambda}}$. Then the velocities can be integrated by inserting $\tilde{\boldsymbol{\lambda}}$ into (18b). Inserting the obtained velocities into (18a) we finally can integrate the positions. The LSE obtained by inserting (18b) into (18c) and dividing by δt is

$$\frac{1}{\delta t}\boldsymbol{g}(\tilde{\boldsymbol{q}}, \tilde{\boldsymbol{\varphi}}) + \delta t \mathbf{J}(\tilde{\boldsymbol{q}}, \tilde{\boldsymbol{\varphi}}) \tilde{\mathbf{M}}^{-1} \mathbf{J}(\tilde{\boldsymbol{q}}, \tilde{\boldsymbol{\varphi}})^T \tilde{\boldsymbol{\lambda}} + \mathbf{J}(\tilde{\boldsymbol{q}}, \tilde{\boldsymbol{\varphi}}) \left(\begin{pmatrix} \tilde{\boldsymbol{v}} \\ \tilde{\boldsymbol{\omega}} \end{pmatrix} + \delta t \tilde{\mathbf{M}}^{-1} \begin{pmatrix} \tilde{\boldsymbol{f}} \\ \tilde{\boldsymbol{\tau}} - \tilde{\boldsymbol{\omega}} \times \tilde{\boldsymbol{\Theta}}\tilde{\boldsymbol{\omega}} \end{pmatrix} \right) = \mathbf{0}. \tag{19}$$

2.4 Dynamic Friction

The table is assumed to slide on the plane, meaning it has nonzero velocity at all times and thus *dynamic* friction is present. This means the friction exactly opposes the tangential relative velocity $\dot{\boldsymbol{g}}_{\boldsymbol{i}_{t,o}}(\boldsymbol{q}(t), \boldsymbol{\varphi}(t))$ at the contacts. The magnitude of the friction force at contact i is the friction coefficient μ_i times the normal reaction force λ_{i_n}. This results in the following expressions for the tangential Lagrange multipliers:

$$\boldsymbol{\lambda}_{\boldsymbol{i}_{t,o}} = -\mu_i(t)\lambda_{i_n} \frac{\dot{\boldsymbol{g}}_{\boldsymbol{i}_{t,o}}(\boldsymbol{q}(t), \boldsymbol{\varphi}(t))}{\|\dot{\boldsymbol{g}}_{\boldsymbol{i}_{t,o}}(\boldsymbol{q}(t), \boldsymbol{\varphi}(t))\|_2} \tag{20}$$

Thus we can express the Lagrange multipliers in terms of the normal components only:

$$\boldsymbol{\lambda} = \begin{bmatrix} 1 & & \\ -\mu_1(t)\frac{\dot{g}_{1_t}(\boldsymbol{q}(t),\boldsymbol{\varphi}(t))}{\|\dot{\boldsymbol{g}}_{\mathbf{1}_{t,o}}(\boldsymbol{q}(t),\boldsymbol{\varphi}(t))\|_2} & & \\ -\mu_1(t)\frac{\dot{g}_{1_t}(\boldsymbol{q}(t),\boldsymbol{\varphi}(t))}{\|\dot{\boldsymbol{g}}_{\mathbf{1}_{t,o}}(\boldsymbol{q}(t),\boldsymbol{\varphi}(t))\|_2} & & \\ & \ddots & \\ & & 1 \\ & & -\mu_4(t)\frac{\dot{g}_{4_t}(\boldsymbol{q}(t),\boldsymbol{\varphi}(t))}{\|\dot{\boldsymbol{g}}_{\mathbf{4}_{t,o}}(\boldsymbol{q}(t),\boldsymbol{\varphi}(t))\|_2} \\ & & -\mu_4(t)\frac{\dot{g}_{4_t}(\boldsymbol{q}(t),\boldsymbol{\varphi}(t))}{\|\dot{\boldsymbol{g}}_{\mathbf{4}_{t,o}}(\boldsymbol{q}(t),\boldsymbol{\varphi}(t))\|_2} \end{bmatrix} \begin{pmatrix} \lambda_{1_n} \\ \lambda_{2_n} \\ \lambda_{3_n} \\ \lambda_{4_n} \end{pmatrix} = \mathbf{K}(\boldsymbol{q}(t),\boldsymbol{\varphi}(t),\boldsymbol{v}(t),\boldsymbol{\omega}(t))\boldsymbol{\lambda_n} \quad (21)$$

Discretizing and inserting this expression for $\tilde{\boldsymbol{\lambda}}$ into Eq. (18) and discarding the rows corresponding to the tangential constraints in the algebraic equations we arrive at the final DAE discretization

$$\begin{pmatrix} \tilde{\boldsymbol{q}}' \\ \tilde{\boldsymbol{\varphi}}' \end{pmatrix} = \delta t \begin{pmatrix} \tilde{\boldsymbol{v}}' \\ \mathbf{Q}(\tilde{\boldsymbol{\varphi}})\tilde{\boldsymbol{\omega}}' \end{pmatrix} + \begin{pmatrix} \tilde{\boldsymbol{q}} \\ \tilde{\boldsymbol{\varphi}} \end{pmatrix} \quad (22a)$$

$$\begin{pmatrix} \tilde{\boldsymbol{v}}' \\ \tilde{\boldsymbol{\omega}}' \end{pmatrix} = \delta t \tilde{\mathbf{M}}^{-1} \begin{pmatrix} \tilde{\boldsymbol{f}} \\ \tilde{\boldsymbol{\tau}} - \tilde{\boldsymbol{\omega}} \times \tilde{\boldsymbol{\Theta}}\tilde{\boldsymbol{\omega}} \end{pmatrix} + \delta t \tilde{\mathbf{M}}^{-1} \mathbf{J}(\tilde{\boldsymbol{q}},\tilde{\boldsymbol{\varphi}})^T \tilde{\mathbf{K}}\tilde{\boldsymbol{\lambda}}_{\boldsymbol{n}} + \begin{pmatrix} \tilde{\boldsymbol{v}} \\ \tilde{\boldsymbol{\omega}} \end{pmatrix} \quad (22b)$$

$$\boldsymbol{g_n}(\tilde{\boldsymbol{q}}',\tilde{\boldsymbol{\varphi}}') = \boldsymbol{g_n}(\tilde{\boldsymbol{q}},\tilde{\boldsymbol{\varphi}}) + \delta t \mathbf{J}_{\boldsymbol{n}*}(\tilde{\boldsymbol{q}},\tilde{\boldsymbol{\varphi}}) \begin{pmatrix} \tilde{\boldsymbol{v}}' \\ \tilde{\boldsymbol{\omega}}' \end{pmatrix} = \mathbf{0} \quad (22c)$$

Inserting Eq. (22b) into Eq. (22c), results in the LSE

$$\frac{1}{\delta t}\boldsymbol{g_n}(\tilde{\boldsymbol{q}},\tilde{\boldsymbol{\varphi}}) + \delta t \mathbf{J}_{\boldsymbol{n}*}(\tilde{\boldsymbol{q}},\tilde{\boldsymbol{\varphi}})\tilde{\mathbf{M}}^{-1}\mathbf{J}(\tilde{\boldsymbol{q}},\tilde{\boldsymbol{\varphi}})^T\tilde{\mathbf{K}}\tilde{\boldsymbol{\lambda}}_{\boldsymbol{n}} + \mathbf{J}_{\boldsymbol{n}*}(\tilde{\boldsymbol{q}},\tilde{\boldsymbol{\varphi}}) \left(\begin{pmatrix} \tilde{\boldsymbol{v}} \\ \tilde{\boldsymbol{\omega}} \end{pmatrix} + \delta t \tilde{\mathbf{M}}^{-1} \begin{pmatrix} \tilde{\boldsymbol{f}} \\ \tilde{\boldsymbol{\tau}} - \tilde{\boldsymbol{\omega}} \times \tilde{\boldsymbol{\Theta}}\tilde{\boldsymbol{\omega}} \end{pmatrix} \right) = \mathbf{0}. \quad (23)$$

3 Numerical Experiments

In order to demonstrate the ill-posedness we simulate a table initially sliding on the ground subject to gravity and dynamic friction. Neighboring coefficients of friction differ and coefficients diagonally across are the same. We number the contacts on the ground in a clockwise fashion and choose the coefficients of friction to be $\boldsymbol{\mu} = (0.1, 0.05, 0.1, 0.05)^T$. The table has unit mass and a unit inertia tensor. The center of mass is assumed to be in the middle between the four legs at height $\frac{1}{2}$, neighboring legs are assumed to be unit length apart. Gravity acts along the negative z-axis and has unit magnitude. The table has an initial velocity of unit magnitude in the x direction. We choose time steps of constant size $\delta t = 0.01$ and simulate until 20 time units have passed. In each time step Eq. (23) is solved using a Moore-Penrose pseudoinverse, which yields the solution of *minimum norm* among the infinite number of solutions of this underdetermined LSE. The minimum norm solution fulfills the non-negativity constraint by assertion. The dotted lines in Fig. 2 show the simulation results when always choosing the minimum norm solution. In order to generate time evolutions of the system, where more or less energy is dissipated, the null space of the system matrix is computed. The dimension of the null space is always 1. Hence we add a multiple of the null space to the minimum norm solution such that the non-negativity constraints are not violated. The factor depends on the desired type of solution. If we intend to minimize the energy in the system, we should minimize the normal reaction at the legs with the smaller coefficient of friction.

Hence we choose the scalar factor such that one of the normal reactions vanishes at the contacts with the smaller coefficients of friction and such that none of the non-negativity constraints are violated. Maximizing the energy, that is minimizing the dissipation, works analogously. The solution minimizing the energy is plotted with solid lines and the solution maximizing the energy is plotted with dashed lines in Fig. 2.

The results clearly show the non-uniqueness of the positions and velocities. For example the time until static friction kicks in rises from the energy minimizing solution, the minimum norm solution to the energy maximizing solution. Also the energy of the minimum norm solution is strictly between the energy of the other solutions.

4 Rigidity as Stiff Limit of Constraint Springs

4.1 Bilateral Joints

These results raise the question: Which one is the solution we look for? In order to approach the answer let us consider what happens when inserting a spring at each contact and let us also treat the contacts as bilateral joints for the moment (say the table is glued to the ground). Instead of requiring the gaps to vanish, we postulate a spring at each joint. Hooke's law provides the relation between displacements and restoring forces

$$\boldsymbol{\lambda} = -\operatorname{diag}(\boldsymbol{k})\boldsymbol{g}(\boldsymbol{q}(t), \boldsymbol{\varphi}(t)), \tag{24}$$

where $\boldsymbol{k}$ is the vector of all spring constants. Note that $\boldsymbol{g}(\boldsymbol{q}(t), \boldsymbol{\varphi}(t))$ is no longer required to be strictly $\mathbf{0}$. Discretizing Eq. (24) *implicitly* leads to

$$\tilde{\boldsymbol{\lambda}} = -\operatorname{diag}(\boldsymbol{k})\boldsymbol{g}(\tilde{\boldsymbol{q}}', \tilde{\boldsymbol{\varphi}}') \tag{25a}$$

$$\overset{(18c)}{=} -\operatorname{diag}(\boldsymbol{k})\left(\boldsymbol{g}(\tilde{\boldsymbol{q}}, \tilde{\boldsymbol{\varphi}}) + \delta t \mathbf{J}(\tilde{\boldsymbol{q}}', \tilde{\boldsymbol{\varphi}}')\begin{pmatrix} \tilde{\boldsymbol{v}}' \\ \tilde{\boldsymbol{\omega}}' \end{pmatrix}\right) \tag{25b}$$

$$\overset{(18b)}{=} -\operatorname{diag}(\boldsymbol{k})\left(\boldsymbol{g}(\tilde{\boldsymbol{q}}, \tilde{\boldsymbol{\varphi}}) + \delta t^2 \mathbf{J}(\tilde{\boldsymbol{q}}, \tilde{\boldsymbol{\varphi}})\tilde{\mathbf{M}}^{-1}\mathbf{J}(\tilde{\boldsymbol{q}}, \tilde{\boldsymbol{\varphi}})^T\tilde{\boldsymbol{\lambda}} + \delta t \mathbf{J}(\tilde{\boldsymbol{q}}, \tilde{\boldsymbol{\varphi}})\left(\begin{pmatrix} \tilde{\boldsymbol{v}} \\ \tilde{\boldsymbol{\omega}} \end{pmatrix} + \delta t \tilde{\mathbf{M}}^{-1}\begin{pmatrix} \tilde{\boldsymbol{f}} \\ \tilde{\boldsymbol{\tau}} - \tilde{\boldsymbol{\omega}} \times \tilde{\boldsymbol{\Theta}}\tilde{\boldsymbol{\omega}} \end{pmatrix}\right)\right). \tag{25c}$$

Rearranging, factoring out $\tilde{\boldsymbol{\lambda}}$ and dividing by δt results in

$$\frac{1}{\delta t}\boldsymbol{g}(\tilde{\boldsymbol{q}}, \tilde{\boldsymbol{\varphi}}) + \delta t\left(\mathbf{J}(\tilde{\boldsymbol{q}}, \tilde{\boldsymbol{\varphi}})\tilde{\mathbf{M}}^{-1}\mathbf{J}(\tilde{\boldsymbol{q}}, \tilde{\boldsymbol{\varphi}})^T + \frac{1}{\delta t^2}\operatorname{diag}(\boldsymbol{k})^{-1}\right)\tilde{\boldsymbol{\lambda}} + \mathbf{J}(\tilde{\boldsymbol{q}}, \tilde{\boldsymbol{\varphi}})\left(\begin{pmatrix} \tilde{\boldsymbol{v}} \\ \tilde{\boldsymbol{\omega}} \end{pmatrix} + \delta t \tilde{\mathbf{M}}^{-1}\begin{pmatrix} \tilde{\boldsymbol{f}} \\ \tilde{\boldsymbol{\tau}} - \tilde{\boldsymbol{\omega}} \times \tilde{\boldsymbol{\Theta}}\tilde{\boldsymbol{\omega}} \end{pmatrix}\right) = \mathbf{0}. \tag{26}$$

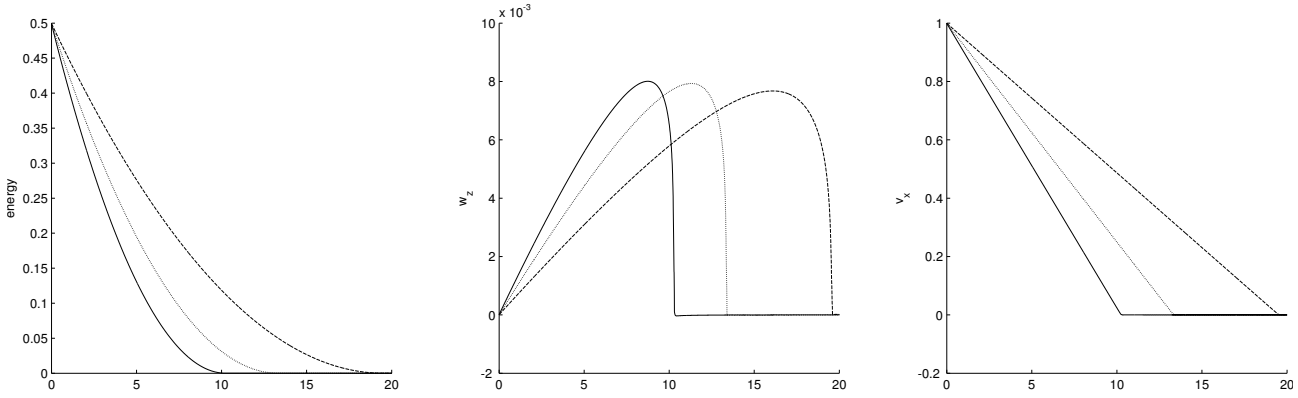

Figure 2: The time evolution of system energy, angular velocity around the ground normal and linear velocity in initial sliding direction of three different impulse solutions.

Note that in the limit when driving $\boldsymbol{k}$ homogeneously towards infinity the diagonal matrix $\text{diag}(\boldsymbol{k})^{-1}$ goes to $\mathbf{0}$ and thus approaches the original formulation Eq. (19). In order to analyze the consequences of this limiting process we introduce a scalar parameter s uniformly scaling the inverse diagonal matrix of spring constants $\mathbf{D} = \text{diag}(\boldsymbol{k})^{-1}$. We also substitute $\mathbf{A}^T\mathbf{A}$ for the system matrix $\mathbf{J}(\tilde{\boldsymbol{q}}, \tilde{\boldsymbol{\varphi}})\tilde{\mathbf{M}}^{-1}\mathbf{J}(\tilde{\boldsymbol{q}}, \tilde{\boldsymbol{\varphi}})^T$[1] and substitute $\boldsymbol{x}$ for $\delta t\tilde{\boldsymbol{\lambda}}$. Furthermore we assume that the gap is currently non-existent that is there is no joint displacement present and thus $\boldsymbol{g}(\tilde{\boldsymbol{q}}, \tilde{\boldsymbol{\varphi}}) = \mathbf{0}$.

$$\mathbf{A}^T\mathbf{A}\boldsymbol{x} - \mathbf{A}^T\boldsymbol{b} = -s\mathbf{D}\boldsymbol{x}. \tag{27}$$

This LSE is known to be equivalent to a damped least squares problem of the following kind:

$$\min_{\boldsymbol{x}} \|\mathbf{A}\boldsymbol{x} - \boldsymbol{b}\|_2^2 + s\boldsymbol{x}^T\mathbf{D}\boldsymbol{x}, \tag{28}$$

The equivalence can be easily shown by calculating the first-order optimality conditions of Eq. (28). The solution of this unconstrained minimization problem approaches for $s \to 0$ the unique solution of the following equality constrained minimization problem as was proved in [6] in detail:

$$\|\mathbf{D}^{\frac{1}{2}}\boldsymbol{x}\|_2^2 = \min_{\boldsymbol{x} \text{ s.t. } \mathbf{A}^T\mathbf{A}\boldsymbol{x}=\mathbf{A}^T\boldsymbol{b}} \boldsymbol{x}^T\mathbf{D}\boldsymbol{x}. \tag{29}$$

In summary this means that we are looking for the *weighted minimum norm solution* of the underdetermined rigid multibody time step problem in the case of bilateral joints.

4.2 Frictionless Unilateral Contacts

For the case of frictionless unilateral contacts we ignore all tangential components of $\boldsymbol{g}$ and only concern ourselves with the normal components identified by an $\boldsymbol{n}$ subscript in the following. A unilateral contact can be in two states in contrast to a bilateral joint: The contact can be closed or it can be open. In the latter case it can either be approaching or separating. Closed contacts act just as bilateral joints however they only take place if the contact reaction is non-negative, that is if it is repulsive. In addition contacts can either be elastic (preserving the energy) or inelastic (dissipative). In the inelastic case energy must be dissipated, which cannot be achieved by a mere spring. Instead an additional damper must be inserted at the contact. The damping force σ_{i_n} opposes the relative contact velocity times the damping coefficient c_{i_n}. Analogously to Eq. (24) we thus obtain

$$g_{i_n}(\boldsymbol{q}(t), \boldsymbol{\varphi}(t)) = -k_{i_n}^{-1}\lambda_{i_n}, \quad \dot{g}_{i_n}(\boldsymbol{q}(t), \boldsymbol{\varphi}(t)) = -c_{i_n}^{-1}\sigma_{i_n}, \quad \lambda_{i_n} \geq 0. \tag{30}$$

Fig. 3 shows the evolution of the gap function $g_{i_n}(\boldsymbol{q}(t), \boldsymbol{\varphi}(t))$ when integrating a point mass under influence of gravity impacting into the ground. If the damping coefficient c_{i_n} is chosen too low then the particle is underdamped and contact is breaking again before enough energy has been dissipated. The dashed line indicates the gap evolution if the contact spring-damper is not removed. The particle would oscillate around the equilibrium with a decreasing amplitude. To avoid underdamping the damping coefficient has to be chosen large enough and then the gap function does not oscillate but approaches the equilibrium from below.

Note that Eq. (30) will always result in penetrations since $g_{i_n}(\boldsymbol{q}(t), \boldsymbol{\varphi}(t))$ must be non-positive due to the non-negativity of λ_{i_n}. Then in contrast the open state of the contact requires that no contact reaction is present meaning no contact spring nor damper is active and that the penetrations are not larger than in the case of the closed contact. This leads to

[1] We can do this because the (inverse) mass matrix is PD and can be decomposed into two factors.

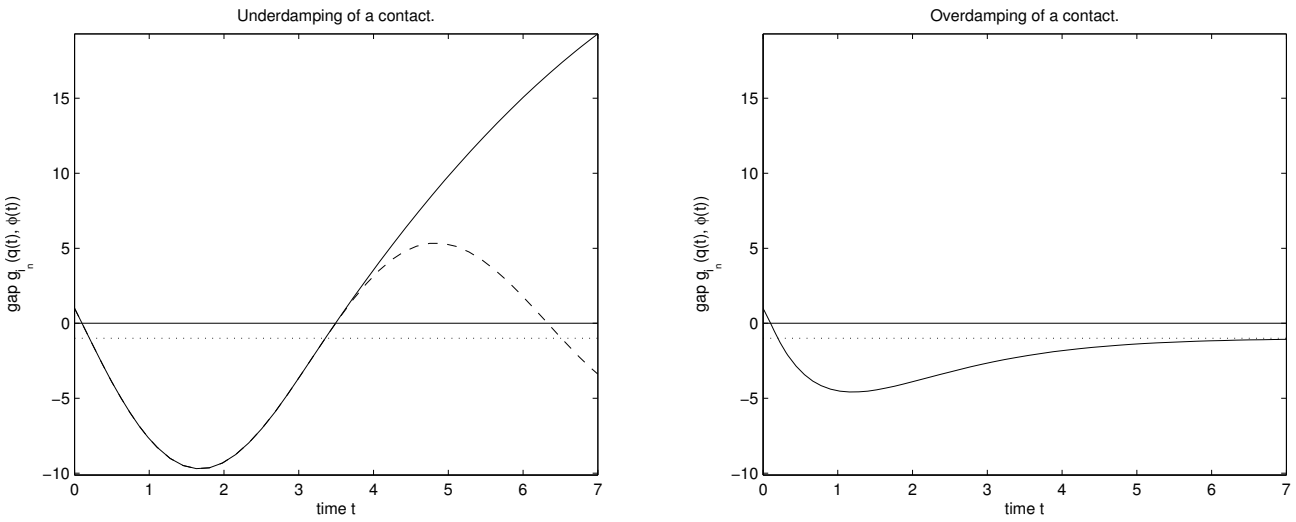

Figure 3: A point mass under the influence of gravity impacting into the ground.

$$g_{i_n}(\boldsymbol{q}(t), \boldsymbol{\varphi}(t)) \geq -k_{i_n}^{-1}\lambda_{i_n}, \quad \lambda_{i_n} = 0, \quad \sigma_{i_n} = 0. \tag{31}$$

Bringing Eq. (30) and Eq. (31) together, rewriting them for the collection of all contacts and deliberately skipping the conditions for the dampers, since we can set them aside as we will see below, one obtains the conditions

$$\boldsymbol{g_n}(\boldsymbol{q}(t), \boldsymbol{\varphi}(t)) + \operatorname{diag}(\boldsymbol{k_n})^{-1}\boldsymbol{\lambda_n} \geq \mathbf{0} \quad \perp \quad \boldsymbol{\lambda_n} \geq \mathbf{0} \tag{32}$$

These conditions can be discretized either implicitly or explicitly. As before we discretize the conditions arising from the spring implicitly leaving out the damping for the moment. Discretizing Eq. (32) implicitly results in

$$\boldsymbol{g_n}(\tilde{\boldsymbol{q}}', \tilde{\boldsymbol{\varphi}}') + \operatorname{diag}(\boldsymbol{k_n})^{-1}\tilde{\boldsymbol{\lambda}}_{\boldsymbol{n}} \geq \mathbf{0} \quad \perp \quad \tilde{\boldsymbol{\lambda}}_{\boldsymbol{n}} \geq \mathbf{0}. \tag{33}$$

Inserting Eq. (18c) and Eq. (18b) results in

$$\begin{aligned}
&\frac{1}{\delta t}\boldsymbol{g_n}(\tilde{\boldsymbol{q}}, \tilde{\boldsymbol{\varphi}}) + \delta t \left(\mathbf{J}_{\boldsymbol{n}*}(\tilde{\boldsymbol{q}}, \tilde{\boldsymbol{\varphi}})\tilde{\mathbf{M}}^{-1}\mathbf{J}_{\boldsymbol{n}*}(\tilde{\boldsymbol{q}}, \tilde{\boldsymbol{\varphi}})^T + \frac{1}{\delta t^2}\operatorname{diag}(\boldsymbol{k_n})^{-1} \right) \tilde{\boldsymbol{\lambda}}_{\boldsymbol{n}} + \\
&\mathbf{J}_{\boldsymbol{n}*}(\tilde{\boldsymbol{q}}, \tilde{\boldsymbol{\varphi}}) \left(\begin{pmatrix} \tilde{\boldsymbol{v}} \\ \tilde{\boldsymbol{\omega}} \end{pmatrix} + \delta t \tilde{\mathbf{M}}^{-1} \begin{pmatrix} \tilde{\boldsymbol{f}} \\ \tilde{\boldsymbol{\tau}} - \tilde{\boldsymbol{\omega}} \times \tilde{\boldsymbol{\Theta}}\tilde{\boldsymbol{\omega}} \end{pmatrix} \right) \geq \mathbf{0} \quad \perp \quad \tilde{\boldsymbol{\lambda}}_{\boldsymbol{n}} \geq \mathbf{0}.
\end{aligned}$$

This LCP is for $\boldsymbol{k_n} \to \infty$ equivalent to methods of Anitescu and Potra [2], which are also based on semi-implicit Euler schemes. However, in this form these schemes produce inelastic impacts even though we left out the dampers in our model. The reason why inelastic impacts are modelled becomes clear when investigating the time evolution of a point mass attached to a support via a spring under the influence of gravity. Fig. 4 shows the time evolution of the displacement for differing spring constants k. The implicit discretization of the spring leads to numerical damping, which gets stronger with increasing spring constant k. Thus for $k \to \infty$ the numerical damping approaches the behaviour of an ideal damper.

Note that even though in the case of the bilateral joint we also did not take dampers into considerations the resulting scheme in the stiff limit is still ideally damped due to the implicit discretization of the spring.

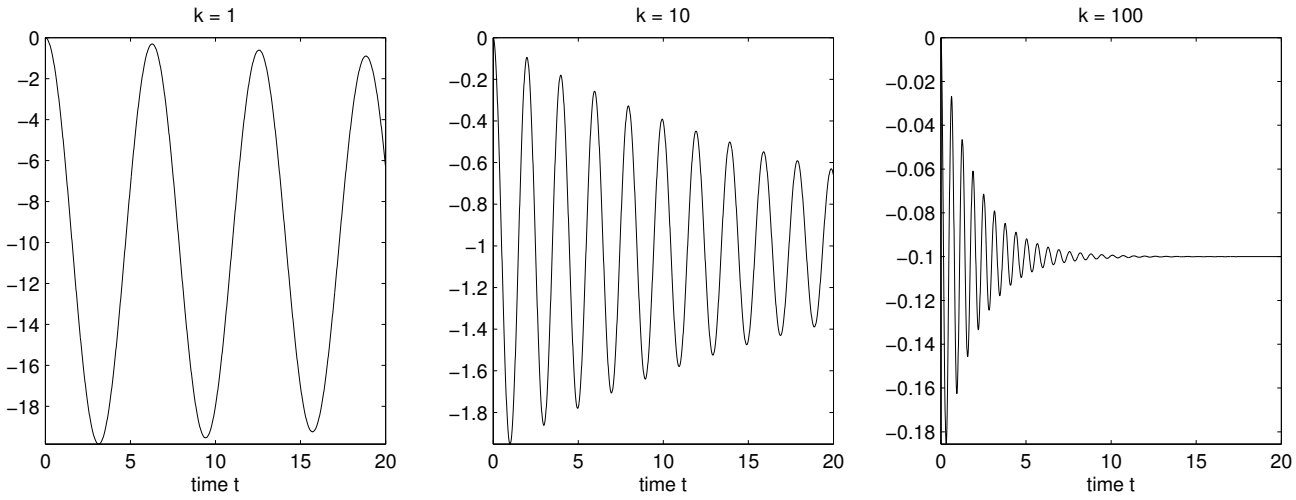

Figure 4: A point mass under the influence of gravity impacting into the ground. Semi-implicit time-integration with implicit springs of varying stiffness.

Applying the same notational simplifications as before and neglecting the current gap $\boldsymbol{g_n}$ leads to a linear complementarity problem (LCP) of the following kind:

$$\mathbf{A}^T\mathbf{A}\boldsymbol{x} - \mathbf{A}^T\boldsymbol{b} \geq -s\mathbf{D}\boldsymbol{x} \quad \perp \quad \boldsymbol{x} \geq \mathbf{0} \tag{34}$$

In [4] it is stated in Th. 5.6.2 that LCPs as the one above have a unique solution for $s > 0$. Under the assumption that $\mathbf{D} = \mathbf{I}$, the solution for a sequence of positive scalars $\{s_\nu\} \to 0$ converges to the minimum norm solution of the unregularized LCP (Eq. (34) where $s = 0$). By substituting $\boldsymbol{x} = \mathbf{D}^{-\frac{1}{2}}\boldsymbol{y}$ and restricting $\mathbf{D}$ to a positive and diagonal matrix one can easily show that the sequence then converges to the weighted minimum norm solution $\boldsymbol{x}^*$

$$\|\mathbf{D}^{\frac{1}{2}}\boldsymbol{x}^*\|_2^2 = \min_{\boldsymbol{x} \text{ s.t. } \mathbf{A}^T\mathbf{A}\boldsymbol{x}-\mathbf{A}^T\boldsymbol{b}\geq\mathbf{0} \ \perp \ \boldsymbol{x}\geq\mathbf{0}} \boldsymbol{x}^T\mathbf{D}\boldsymbol{x}. \tag{35}$$

For completeness we adapted Th. 5.6.2 and its proof from [4] for $\mathbf{D}$ symmetric positive-definite (SPD).

Theorem 4.1. *Let $\mathbf{A}$ be rectangular, $\mathbf{D}$ be a symmetric positive-definite matrix and let $\{s_\nu\}$ be a decreasing sequence of positive scalars with $s_\nu \to 0$. For each ν, let $\boldsymbol{x}_\nu$ be the unique solution of the LCP*

$$(\mathbf{A}^T\mathbf{A} + s_\nu\mathbf{D})\boldsymbol{x}_\nu - \mathbf{A}^T\boldsymbol{b} \geq \mathbf{0} \perp \boldsymbol{x}_\nu \geq \mathbf{0}. \tag{36}$$

Then the sequence $\{\boldsymbol{x}_\nu\}$ converges to the weighted minimum norm solution $\boldsymbol{x}_{wmn}$

$$\|\mathbf{D}^{\frac{1}{2}}\boldsymbol{x}_{wmn}\|_2^2 = \min_{\boldsymbol{x} \ s.t. \ \mathbf{A}^T\mathbf{A}\boldsymbol{x}-\mathbf{A}^T\boldsymbol{b}\geq\mathbf{0} \ \perp \ \boldsymbol{x}\geq\mathbf{0}} \boldsymbol{x}^T\mathbf{D}\boldsymbol{x} \tag{37}$$

Proof. According to [3], page 5 the LCP

$$\mathbf{A}^T\mathbf{A}\boldsymbol{x} - \mathbf{A}^T\boldsymbol{b} \geq \mathbf{0} \perp \boldsymbol{x} \geq \mathbf{0} \tag{38}$$

is completely equivalent with the quadratic program

$$\min_{\boldsymbol{x}\geq\mathbf{0}} \frac{1}{2}\boldsymbol{x}^T\mathbf{A}^T\mathbf{A}\boldsymbol{x} - \boldsymbol{x}^T\mathbf{A}^T\boldsymbol{b} \tag{39}$$

because the matrix $\mathbf{A}^T\mathbf{A}$ is symmetric and positive semidefinite. Thus, the solution set of the problem (38), denoted by SOL (38) is equal with the solution set of the quadratic program (39). Let now $\boldsymbol{x}^* \in \mathbb{R}^n$ be an arbitrary fixed solution of the normal equation $\mathbf{A}^T\mathbf{A}\boldsymbol{x}^* = \mathbf{A}^T\boldsymbol{b}$. A simple computation gives us the inequality

$$\frac{1}{2}\langle\mathbf{A}^T\mathbf{A}(\boldsymbol{x}^* + \lambda\boldsymbol{x}), \boldsymbol{x}^* + \lambda\boldsymbol{x}\rangle - \langle\mathbf{A}^T\boldsymbol{b}, \boldsymbol{x}^* + \lambda\boldsymbol{x}\rangle \geq \frac{1}{2}\langle\mathbf{A}^T\mathbf{A}\boldsymbol{x}^*, \boldsymbol{x}^*\rangle - \langle\mathbf{A}^T\boldsymbol{b}, \boldsymbol{x}^*\rangle,$$

for all $\boldsymbol{x} \in \mathbb{R}^n$ and $\lambda \in \mathbb{R}$. This tells us that the quadratic function from (39) is bounded from below in $\mathbb{R}^n$ and thus in the non-negative orthant of $\mathbb{R}^n$. Then, with classical arguments we conclude that at least one solution exists for the problem (39) and thus for (38), i.e. SOL (38) is nonempty. We will show that it is also closed. Indeed the problem (38) can be written as

$$\boldsymbol{x} \geq \mathbf{0},\ \mathbf{A}^T\mathbf{A}\boldsymbol{x} - \mathbf{A}^T\boldsymbol{b} \geq \mathbf{0} \text{ and } \langle \boldsymbol{x}, \mathbf{A}^T\mathbf{A}\boldsymbol{x} - \mathbf{A}^T\boldsymbol{b}\rangle = 0, \tag{40}$$

Then let $(\boldsymbol{x}_k)_{k\geq 0}$ be a sequence of solutions for (38) such that $\exists \lim_{k\to\infty} \boldsymbol{x}_k = \boldsymbol{x}^*$. Each $\boldsymbol{x}_k$ satisfies (40), thus by taking limits we get that also $\boldsymbol{x}^*$ verifies those relations, i.e. $\boldsymbol{x}^* \in \text{SOL}\,(38) \neq \emptyset$.

Concerning the LCP (36), for any $s_\nu > 0$ it has a unique solution $\boldsymbol{x}_\nu$ according to Th. 3.1.6 on page 141 in [3] because the matrix $\mathbf{A}^T\mathbf{A} + s_\nu\mathbf{D}$ is SPD.

Now, let us consider the function $f : \text{SOL}\,(38) \to \mathbb{R}, f(\boldsymbol{x}) = \|\mathbf{D}^{\frac{1}{2}}\boldsymbol{x}\|_2$. Because $f(\boldsymbol{x}) \geq 0, \forall \boldsymbol{x} \in \text{SOL}\,(38)$ there exists a minimum $m_0 = \min_{\boldsymbol{x}\in\text{SOL}\,(38)} f(\boldsymbol{x})$ and a sequence $(\boldsymbol{x}_k)_{k\geq 0} \subset \text{SOL}\,(38)$ sucht that $m_0 = \lim_{k\to\infty} f(\boldsymbol{x}_k)$ and the sequence $(f(\boldsymbol{x}_k))_{k\geq 0}$ is decreasing, i.e.

$$f(\boldsymbol{x}_0) \geq \cdots \geq f(\boldsymbol{x}_k) \geq f(\boldsymbol{x}_{k+1}), \forall k \geq 0. \tag{41}$$

From (41) it results that the sequence $(f(\boldsymbol{x}_k))_{k\geq 0} = (\|\mathbf{D}^{\frac{1}{2}}\boldsymbol{x}_k\|_2)_{k\geq 0} = (\|\boldsymbol{x}_k\|_{\mathbf{D}})_{k\geq 0}$ is bounded, so will be $(\|\boldsymbol{x}_k\|_2)_{k\geq 0}$ (because any two norms on $\mathbb{R}^n$ are equivalent, thus also the Euclidean $\|\cdot\|_2$ and the energy norm $\|\cdot\|_{\mathbf{D}}$) and $(\boldsymbol{x}_k)_{k\geq 0}$ (by the definition of boundedness in $\mathbb{R}^n$). Because one can extract a convergent subsequence from any bounded sequence, it will then exist at least a convergent subsequence $(\boldsymbol{x}_{k_r})_{r\geq 0}$ of $(\boldsymbol{x}_k)_{k\geq 0}$, i.e.

$$\lim_{r\to\infty} \boldsymbol{x}_{k_r} = \bar{\boldsymbol{x}} \in \text{SOL}\,(38), \tag{42}$$

because SOL (38) is closed. Thus, we found a solution for (37).

The solution of (37) is unique. This can be seen by noting that the objective function of (37) is strictly convex because $\mathbf{D}$ is PD and that the constraint set is convex too. That SOL (38) is convex in the PSD case can be concluded from [3], Th. 3.1.7 (a), Eq. (11), on page 141 combined with Th. 3.1.8 (b), on page 144. Thus (37) is a strictly convex quadratic program, and as it is well known strictly convex programs have unique solutions on convex domains.

Now, we will adapt the procedure in the proof of part (b) of Th. 5.6.2 from [3]. Consider the vectors $\boldsymbol{x}_\nu$ – the unique solution of the problem (36), $\tilde{\boldsymbol{x}}$ – a solution of the problem (38), and $\tilde{\boldsymbol{w}}$, $\boldsymbol{w}_\nu$ defined by

$$\tilde{\boldsymbol{w}} = \mathbf{A}^T\mathbf{A}\tilde{x} - \mathbf{A}^T\boldsymbol{b}, \quad \boldsymbol{w}_\nu = \mathbf{A}^T\mathbf{A}\boldsymbol{x}_\nu + s_\nu\mathbf{D}\boldsymbol{x}_\nu - \mathbf{A}^T\boldsymbol{b}. \tag{43}$$

Because $\langle \boldsymbol{x}_\nu, \boldsymbol{w}_\nu\rangle = 0$, $\langle \tilde{\boldsymbol{x}}, \tilde{\boldsymbol{w}}\rangle = 0$ and $\langle \boldsymbol{x}_\nu, \tilde{\boldsymbol{w}}\rangle \geq 0$, $\langle \tilde{\boldsymbol{x}}, \boldsymbol{w}_\nu\rangle \geq 0$ we get

$$0 \geq \langle \boldsymbol{x}_\nu - \tilde{\boldsymbol{x}}, \boldsymbol{w}_\nu - \tilde{\boldsymbol{w}}\rangle = \langle \boldsymbol{x}_\nu - \tilde{\boldsymbol{x}}, \mathbf{A}^T\mathbf{A}(\boldsymbol{x}_\nu - \tilde{\boldsymbol{x}})\rangle +$$

$$s_\nu\langle \boldsymbol{x}_\nu - \tilde{\boldsymbol{x}}, \mathbf{D}\boldsymbol{x}_\nu\rangle \geq s_\nu\langle \boldsymbol{x}_\nu - \tilde{\boldsymbol{x}}, \mathbf{D}\boldsymbol{x}_\nu\rangle. \tag{44}$$

Thus, from the fact that the last expression in (44) is non-positive we get

$$\|\mathbf{D}^{\frac{1}{2}}\boldsymbol{x}_\nu\|_2^2 = \langle \boldsymbol{x}_\nu, \mathbf{D}\boldsymbol{x}_\nu\rangle \leq \langle \tilde{\boldsymbol{x}}, \mathbf{D}\boldsymbol{x}_\nu\rangle =$$
$$\langle \mathbf{D}^{\frac{1}{2}}\tilde{\boldsymbol{x}}, \mathbf{D}^{\frac{1}{2}}\boldsymbol{x}_\nu\rangle \leq \|\mathbf{D}^{\frac{1}{2}}\tilde{\boldsymbol{x}}\|_2\|\mathbf{D}^{\frac{1}{2}}\boldsymbol{x}_\nu\|_2,$$

i.e.

$$\|\mathbf{D}^{\frac{1}{2}}\boldsymbol{x}_\nu\|_2 \leq \|\mathbf{D}^{\frac{1}{2}}\tilde{\boldsymbol{x}}\|_2,\ \forall \nu \geq 0. \tag{45}$$

From (45) it results that the sequence $(\boldsymbol{x}_\nu)_{\nu\geq 0}$ is bounded, thus it exists at least one convergent subsequence $(\boldsymbol{x}_{\nu_r})_{r\geq 0}$, $\lim_{r\to\infty} \boldsymbol{x}_{\nu_r} = \boldsymbol{x}^* \in \text{SOL}\,(38)$. The limit point $\boldsymbol{x}^*$ has the property that

$$\|\mathbf{D}^{\frac{1}{2}}\boldsymbol{x}^*\|_2 \leq \|\mathbf{D}^{\frac{1}{2}}\boldsymbol{x}\|_2,\ \forall \boldsymbol{x} \in \text{SOL}\,(38). \tag{46}$$

As in [3] it then follows that every accumulation point of the sequence $(\boldsymbol{x}_\nu)_{\nu\geq 0}$ is equal to the unique weighted minimum norm solution $\boldsymbol{x}_{wmn}$. Thus, as in Th. 5.6.2 from [3] we get

$$\lim_{\nu\to\infty} \boldsymbol{x}_\nu = \boldsymbol{x}_{wmn}. \tag{47}$$

□

4.3 Pseudo-Frictional Unilateral Contacts

Here pseudo-friction shall be defined as not depending on the unknown normal reaction. Instead it is assumed that a reasonable approximation $\bar{\boldsymbol{\lambda}}_{\boldsymbol{n}}$ is known a priori and applied to compute the friction limits, which would normally depend on the normal reaction. In contrast to the frictionless unilateral contact we must take care of the tangential components of $\boldsymbol{g}$ identified by $\boldsymbol{t}$ and $\boldsymbol{o}$ subscripts in the following. The two states are now replaced by three states, one of them still being an *open* contact, where no contact reaction, neither in normal nor in tangential direction, is present. However, a closed contact may now be either *static* or *dynamic*, that is friction can either hold the contact in place or the friction would need to exceed its limits to hold it in place, in which case the friction must do its utmost to prevent sliding. The conditions for a static contact can be extended in a straight-forward manner from Eq. (30) by also introducing a spring-damper in tangential direction.

$$g_{i_n}(\boldsymbol{q}(t),\boldsymbol{\varphi}(t)) = -k_{i_n}^{-1}\lambda_{i_n}, \qquad \dot{g}_{i_n}(\boldsymbol{q}(t),\boldsymbol{\varphi}(t)) = -c_{i_n}^{-1}\sigma_{i_n}, \qquad \lambda_{i_n} \geq 0 \tag{48a}$$

$$\boldsymbol{g}_{\boldsymbol{i}_{t,o}}(\boldsymbol{q}(t),\boldsymbol{\varphi}(t)) = -\operatorname{diag}(\boldsymbol{k}_{\boldsymbol{i}_{t,o}})^{-1}\boldsymbol{\lambda}_{\boldsymbol{i}_{t,o}}, \quad \dot{\boldsymbol{g}}_{\boldsymbol{i}_{t,o}}(\boldsymbol{q}(t),\boldsymbol{\varphi}(t)) = -\operatorname{diag}(\boldsymbol{c}_{\boldsymbol{i}_{t,o}})^{-1}\boldsymbol{\sigma}_{\boldsymbol{i}_{t,o}}, \quad \|\boldsymbol{\lambda}_{\boldsymbol{i}_{t,o}}\|_2 \leq \mu_i(t)\bar{\lambda}_{i_n}. \tag{48b}$$

Also the open contact is easily extended from Eq. (31) since no friction can act when no normal reaction is present:

$$g_{i_n}(\boldsymbol{q}(t),\boldsymbol{\varphi}(t)) \geq -k_{i_n}^{-1}\lambda_{i_n}, \quad \lambda_{i_n} = \lambda_{i_t} = \lambda_{i_o} = 0, \quad \sigma_{i_n} = \sigma_{i_t} = \sigma_{i_o} = 0. \tag{49}$$

The third state to be defined is the dynamic closed contact. As it was already done and explained in Sec. 2.4 the dynamic friction force has to exactly oppose the slip $\dot{\boldsymbol{g}}_{\boldsymbol{i}_{t,o}}(\boldsymbol{q}(t),\boldsymbol{\varphi}(t))$ and has magnitude $\mu_i(t)\lambda_{i_n}$. This indicates that dynamic friction involves a limited damper and not a spring as in the static case. However there is one subtle pitfall: Contact points do not move along with the actual contacting point! For dynamic contacts the two points involved in a contact drift apart and promptly another contact point replaces the previous. Thus for *closed contacts* we can always assume that $\boldsymbol{g}_{\boldsymbol{i}_{t,o}}(\boldsymbol{q}(t),\boldsymbol{\varphi}(t)) = \boldsymbol{0}$. From this we can derive

$$\begin{aligned}\frac{\dot{\boldsymbol{g}}(\boldsymbol{q}(t),\boldsymbol{\varphi}(t))_{\boldsymbol{i}_{t,o}}}{\|\dot{\boldsymbol{g}}(\boldsymbol{q}(t),\boldsymbol{\varphi}(t))_{\boldsymbol{i}_{t,o}}\|_2} &= \lim_{\epsilon\to 0} \frac{\frac{\boldsymbol{g}(\boldsymbol{q}(t+\epsilon),\boldsymbol{\varphi}(t+\epsilon))_{\boldsymbol{i}_{t,o}} - \boldsymbol{g}(\boldsymbol{q}(t),\boldsymbol{\varphi}(t))_{\boldsymbol{i}_{t,o}}}{\epsilon}}{\|\frac{\boldsymbol{g}(\boldsymbol{q}(t+\epsilon),\boldsymbol{\varphi}(t+\epsilon))_{\boldsymbol{i}_{t,o}} - \boldsymbol{g}(\boldsymbol{q}(t),\boldsymbol{\varphi}(t))_{\boldsymbol{i}_{t,o}}}{\epsilon}\|_2} \\ &= \lim_{\epsilon\to 0} \frac{\boldsymbol{g}(\boldsymbol{q}(t+\epsilon),\boldsymbol{\varphi}(t+\epsilon))_{\boldsymbol{i}_{t,o}}}{\|\boldsymbol{g}(\boldsymbol{q}(t+\epsilon),\boldsymbol{\varphi}(t+\epsilon))_{\boldsymbol{i}_{t,o}}\|_2} = \frac{\boldsymbol{g}(\boldsymbol{q}(t),\boldsymbol{\varphi}(t))_{\boldsymbol{i}_{t,o}}}{\|\boldsymbol{g}(\boldsymbol{q}(t),\boldsymbol{\varphi}(t))_{\boldsymbol{i}_{t,o}}\|_2}.\end{aligned} \tag{50}$$

Hence the conditions for a dynamic closed contact are

$$g_{i_n}(\boldsymbol{q}(t),\boldsymbol{\varphi}(t)) = -k_{i_n}^{-1}\lambda_{i_n}, \qquad \dot{g}_{i_n}(\boldsymbol{q}(t),\boldsymbol{\varphi}(t)) = -c_{i_n}^{-1}\sigma_{i_n}, \qquad \lambda_{i_n} \geq 0 \tag{51a}$$

$$\boldsymbol{\lambda}_{\boldsymbol{i}_{t,o}} = -\frac{\boldsymbol{g}_{\boldsymbol{i}_{t,o}}(\boldsymbol{q}(t),\boldsymbol{\varphi}(t))}{\|\boldsymbol{g}_{\boldsymbol{i}_{t,o}}(\boldsymbol{q}(t),\boldsymbol{\varphi}(t))\|_2}\mu_i(t)\bar{\lambda}_{i_n}, \quad \dot{\boldsymbol{g}}_{\boldsymbol{i}_{t,o}}(\boldsymbol{q}(t),\boldsymbol{\varphi}(t)) = -\operatorname{diag}(\boldsymbol{c}_{\boldsymbol{i}_{t,o}})^{-1}\boldsymbol{\sigma}_{\boldsymbol{i}_{t,o}}, \quad \|\boldsymbol{\lambda}_{\boldsymbol{i}_{t,o}}\|_2 = \mu_i(t)\bar{\lambda}_{i_n} \tag{51b}$$

and in contrast to Eq. (20) the friction is now consistently a spring, for static as well as dynamic friction, whose restoring force is limited by $\mu_i(t)\bar{\lambda}_{i_n}$.

Analogously to the formulation in Eq. (5) we can summarize all frictional constraints into a two-dimensional complementarity constraint in addition to the one-dimensional complementarity constraint of the normal reaction. We will deliberately skip the damping again since it will be introduced artificially by the discretization as before.

$$g_{i_n}(\boldsymbol{q}(t), \boldsymbol{\varphi}(t)) + k_{i_n}^{-1}\lambda_{i_n} \geq 0 \quad \perp \quad \lambda_{i_n} \geq 0 \tag{52a}$$

$$\boldsymbol{g}_{\boldsymbol{i}_{t,o}}(\boldsymbol{q}(t), \boldsymbol{\varphi}(t)) + \operatorname{diag}(\boldsymbol{k}_{\boldsymbol{i}_{t,o}})^{-1}\boldsymbol{\lambda}_{\boldsymbol{i}_{t,o}} \in \mathcal{N}_{\mathcal{S}(\mu_i(t)\bar{\lambda}_{i_n})}(\boldsymbol{\lambda}_{\boldsymbol{i}_{t,o}}) \quad \perp \quad \boldsymbol{\lambda}_{\boldsymbol{i}_{t,o}} \in \mathcal{S}(\mu_i(t)\bar{\lambda}_{i_n}) \tag{52b}$$

Note that Eq. (52b) is indeed equivalent to Eq. (48b) and Eq. (51b). If the contact is static then $\boldsymbol{\lambda}_{\boldsymbol{i}_{t,o}}$ is in the inside of the disc $\mathcal{S}(\mu_i(t)\bar{\lambda}_{i_n})$. Thus the normal cone $\mathcal{N}_{\mathcal{S}(\mu_i(t)\bar{\lambda}_{i_n})}$ degenerates to the set $\{\mathbf{0}\}$ and Eq. (48b) is recovered. In case of dynamic friction the friction force is located on the boundary of the disc $\boldsymbol{\lambda}_{\boldsymbol{i}_{t,o}} \in \partial\mathcal{S}(\mu_i(t)\bar{\lambda}_{i_n})$ and the normal cone is the ray pointing in the direction opposite to $\boldsymbol{\lambda}_{\boldsymbol{i}_{t,o}}$ and thus

$$\boldsymbol{g}_{\boldsymbol{i}_{t,o}}(\boldsymbol{q}(t), \boldsymbol{\varphi}(t)) + \operatorname{diag}(\boldsymbol{k}_{\boldsymbol{i}_{t,o}})^{-1}\boldsymbol{\lambda}_{\boldsymbol{i}_{t,o}} = -C_1\boldsymbol{\lambda}_{\boldsymbol{i}_{t,o}}, \quad C_1 \geq 0 \tag{53a}$$

$$\boldsymbol{g}_{\boldsymbol{i}_{t,o}}(\boldsymbol{q}(t), \boldsymbol{\varphi}(t)) + (\operatorname{diag}(\boldsymbol{k}_{\boldsymbol{i}_{t,o}})^{-1} + C_1)\boldsymbol{\lambda}_{\boldsymbol{i}_{t,o}} = \mathbf{0} \tag{53b}$$

Under the assumption that $k_{i_t} = k_{i_o} = C_2$, which is reasonable for isotropic friction this can be transformed to

$$\boldsymbol{\lambda}_{\boldsymbol{i}_{t,o}} = -\frac{1}{C_2^{-1} + C_1}\boldsymbol{g}_{\boldsymbol{i}_{t,o}}(\boldsymbol{q}(t), \boldsymbol{\varphi}(t)). \tag{54}$$

Since the contact is dynamic and thus $\|\boldsymbol{\lambda}_{\boldsymbol{i}_{t,o}}\|_2 = \mu_i(t)\bar{\lambda}_{i_n}$ it follows that

$$\|\boldsymbol{\lambda}_{\boldsymbol{i}_{t,o}}\|_2 = \frac{1}{C_2^{-1} + C_1}\|\boldsymbol{g}_{\boldsymbol{i}_{t,o}}(\boldsymbol{q}(t), \boldsymbol{\varphi}(t))\|_2 \stackrel{!}{=} \mu_i(t)\bar{\lambda}_{i_n} \tag{55}$$

and thus

$$\boldsymbol{\lambda}_{\boldsymbol{i}_{t,o}} = -\mu_i(t)\bar{\lambda}_{i_n}\frac{\boldsymbol{g}_{\boldsymbol{i}_{t,o}}(\boldsymbol{q}(t), \boldsymbol{\varphi}(t))}{\|\boldsymbol{g}_{\boldsymbol{i}_{t,o}}(\boldsymbol{q}(t), \boldsymbol{\varphi}(t))\|_2}, \tag{56}$$

which recovers Eq. (51b).

Eq. (52) can be reformulated into a variational inequality (VI) in a straight-forward manner since the bounds do not depend on the unknowns due to the simplification of the pseudo-friction:

$$\lambda_{i_n} \in [0; \infty), \quad (g_{i_n}(\boldsymbol{q}(t), \boldsymbol{\varphi}(t)) + k_{i_n}^{-1}\lambda_{i_n})^T(y_{i_n} - \lambda_{i_n}) \geq 0, \quad \forall y_{i_n} \in [0; \infty) \tag{57a}$$

$$\boldsymbol{\lambda}_{\boldsymbol{i}_{t,o}} \in \mathcal{S}(\mu_i(t)\bar{\lambda}_{i_n}), \quad (\boldsymbol{g}_{\boldsymbol{i}_{t,o}}(\boldsymbol{q}(t), \boldsymbol{\varphi}(t)) + \operatorname{diag}(\boldsymbol{k}_{\boldsymbol{i}_{t,o}})^{-1}\boldsymbol{\lambda}_{\boldsymbol{i}_{t,o}})^T(\boldsymbol{y}_{\boldsymbol{i}_{t,o}} - \boldsymbol{\lambda}_{\boldsymbol{i}_{t,o}}) \geq 0, \quad \forall \boldsymbol{y}_{\boldsymbol{i}_{t,o}} \in \mathcal{S}(\mu_i(t)\bar{\lambda}_{i_n}) \tag{57b}$$

Or rewritten for the collection of all contacts:

$$\boldsymbol{\lambda} \in \mathcal{F}(t) = \prod_i [0; \infty) \times \mathcal{S}(\mu_i(t)\bar{\lambda}_{i_n}), \quad (\boldsymbol{g}(\boldsymbol{q}(t), \boldsymbol{\varphi}(t)) + \operatorname{diag}(\boldsymbol{k})^{-1}\boldsymbol{\lambda})^T(\boldsymbol{y} - \boldsymbol{\lambda}) \geq 0, \quad \forall \boldsymbol{y} \in \mathcal{F}(t). \tag{58}$$

As before we discretize the springs implicitly and arrive at

$$\tilde{\boldsymbol{\lambda}} \in \tilde{\mathcal{F}} = \prod_i [0;\infty) \times \mathcal{S}(\tilde{\mu}_i \bar{\lambda}_{i_n}), \quad (\boldsymbol{g}(\tilde{\boldsymbol{q}}', \tilde{\boldsymbol{\varphi}}') + \operatorname{diag}(\boldsymbol{k})^{-1}\tilde{\boldsymbol{\lambda}})^T(\boldsymbol{y} - \tilde{\boldsymbol{\lambda}}) \geq 0, \quad \forall \boldsymbol{y} \in \tilde{\mathcal{F}}. \tag{59}$$

Inserting Eq. (18c) and Eq. (18b) results in

$$\begin{aligned} \tilde{\boldsymbol{\lambda}} \in \tilde{\mathcal{F}}, \quad & \left(\frac{1}{\delta t} \boldsymbol{g}(\tilde{\boldsymbol{q}}, \tilde{\boldsymbol{\varphi}}) + \delta t \left(\mathbf{J}(\tilde{\boldsymbol{q}}, \tilde{\boldsymbol{\varphi}}) \tilde{\mathbf{M}}^{-1} \mathbf{J}(\tilde{\boldsymbol{q}}, \tilde{\boldsymbol{\varphi}})^T + \frac{1}{\delta t^2} \operatorname{diag}(\boldsymbol{k})^{-1} \right) \tilde{\boldsymbol{\lambda}} + \right. \\ & \left. \mathbf{J}(\tilde{\boldsymbol{q}}, \tilde{\boldsymbol{\varphi}}) \left(\begin{pmatrix} \tilde{\boldsymbol{v}} \\ \tilde{\boldsymbol{\omega}} \end{pmatrix} + \delta t \tilde{\mathbf{M}}^{-1} \begin{pmatrix} \tilde{\boldsymbol{f}} \\ \tilde{\boldsymbol{\tau}} - \tilde{\boldsymbol{\omega}} \times \tilde{\boldsymbol{\Theta}} \tilde{\boldsymbol{\omega}} \end{pmatrix} \right) \right)^T (\boldsymbol{y} - \tilde{\boldsymbol{\lambda}}) \geq 0, \quad \forall \boldsymbol{y} \in \tilde{\mathcal{F}}. \end{aligned} \tag{60}$$

Applying the same notational simplifications as before and neglecting the current gap $\boldsymbol{g}$ leads to a VI of the following kind:

$$\boldsymbol{x} \in \delta t \tilde{\mathcal{F}}, \quad ((\mathbf{A}^T\mathbf{A} + s\mathbf{D})\boldsymbol{x} - \mathbf{A}^T\boldsymbol{b})^T(\boldsymbol{y} - \boldsymbol{x}) \geq 0, \quad \forall \boldsymbol{y} \in \delta t \tilde{\mathcal{F}}. \tag{61}$$

In [8] such a regularized VI was proved to have a unique solution and that as $s \to 0$ its solution converges to a minimum norm solution of the unregularized (where $s = 0$) VI if $\mathbf{D} = \mathbf{I}$. By substituting $\boldsymbol{x} = \mathbf{D}^{-\frac{1}{2}}\boldsymbol{z}$ one can show that the solution converges for $\mathbf{D}$ symmetric positive-definite (SPD) to a weighted minimum norm solution.

$$\begin{aligned} & \boldsymbol{x} \in \delta t \tilde{\mathcal{F}}, \quad ((\mathbf{A}^T\mathbf{A} + s\mathbf{D})\boldsymbol{x} - \mathbf{A}^T\boldsymbol{b})^T(\boldsymbol{y} - \boldsymbol{x}) \geq 0, \quad \forall \boldsymbol{y} \in \delta t \tilde{\mathcal{F}} \\ \overset{[5]}{\leftrightarrow} & \min_{\text{s.t. } \boldsymbol{x} \in \delta t \tilde{\mathcal{F}}} \frac{1}{2}\boldsymbol{x}^T(\mathbf{A}^T\mathbf{A} + s\mathbf{D})\boldsymbol{x} - \boldsymbol{x}^T\mathbf{A}^T\boldsymbol{b} \\ \overset{\boldsymbol{x}=\mathbf{D}^{-\frac{1}{2}}\boldsymbol{z}}{\leftrightarrow} & \min_{\text{s.t. } \mathbf{D}^{-\frac{1}{2}}\boldsymbol{z} \in \delta t \tilde{\mathcal{F}}} \frac{1}{2}\boldsymbol{z}^T\mathbf{D}^{-\frac{T}{2}}(\mathbf{A}^T\mathbf{A} + s\mathbf{D})\mathbf{D}^{-\frac{1}{2}}\boldsymbol{z} - \boldsymbol{z}^T\mathbf{D}^{-\frac{T}{2}}\mathbf{A}^T\boldsymbol{b} \\ \overset{\mathbf{A}\mathbf{D}^{-\frac{1}{2}}=\hat{\mathbf{A}}}{\leftrightarrow} & \min_{\text{s.t. } \boldsymbol{z} \in \delta t \mathbf{D}^{\frac{1}{2}} \tilde{\mathcal{F}}} \frac{1}{2}\boldsymbol{z}^T(\hat{\mathbf{A}}^T\hat{\mathbf{A}} + s\mathbf{I})\boldsymbol{z} - \boldsymbol{z}^T\hat{\mathbf{A}}^T\boldsymbol{b} \\ \overset{[5]}{\leftrightarrow} & \boldsymbol{z} \in \delta t \mathbf{D}^{\frac{1}{2}} \tilde{\mathcal{F}}, \quad ((\hat{\mathbf{A}}^T\hat{\mathbf{A}} + s\mathbf{I})\boldsymbol{z} - \hat{\mathbf{A}}^T\boldsymbol{b})^T(\boldsymbol{y} - \boldsymbol{z}) \geq 0, \quad \forall \boldsymbol{y} \in \delta t \mathbf{D}^{\frac{1}{2}} \tilde{\mathcal{F}} \end{aligned} \tag{62}$$

According to [8] and since $\delta t \mathbf{D}^{\frac{1}{2}} \tilde{\mathcal{F}}$ is still a nonempty closed convex set for $s \to 0$ the solution $\boldsymbol{z}$ converges to the minimum norm solution of the unregularized VI $\boldsymbol{z} \in \delta t \mathbf{D}^{\frac{1}{2}} \tilde{\mathcal{F}}, (\hat{\mathbf{A}}^T\hat{\mathbf{A}}\boldsymbol{z} - \hat{\mathbf{A}}^T\boldsymbol{b})^T(\boldsymbol{y} - \boldsymbol{z}) \geq 0, \forall \boldsymbol{y} \in \delta t \mathbf{D}^{\frac{1}{2}} \tilde{\mathcal{F}}$ and thus when substituting back we obtain that if $\mathbf{D}$ is SPD then $\boldsymbol{x}$ converges to the weighted minimum norm solution of the initial unregularized problem (Eq. (61) with $s = 0$)

$$\min_{\boldsymbol{z} \in \delta t \mathbf{D}^{\frac{1}{2}} \tilde{\mathcal{F}}, (\hat{\mathbf{A}}^T\hat{\mathbf{A}}\boldsymbol{z} - \hat{\mathbf{A}}^T\boldsymbol{b})^T(\boldsymbol{y} - \boldsymbol{z}) \geq 0, \forall \boldsymbol{y} \in \delta t \mathbf{D}^{\frac{1}{2}} \tilde{\mathcal{F}}} \boldsymbol{z}^T\boldsymbol{z} = \min_{\boldsymbol{x} \in \delta t \tilde{\mathcal{F}}, (\mathbf{A}^T\mathbf{A}\boldsymbol{x} - \mathbf{A}^T\boldsymbol{b})^T(\boldsymbol{y} - \boldsymbol{x}) \geq 0, \forall \boldsymbol{y} \in \delta t \tilde{\mathcal{F}}} \boldsymbol{x}^T\mathbf{D}\boldsymbol{x}. \tag{63}$$

Note that this proof includes LCPs as a special case for $\tilde{\mathcal{F}} = \prod_i [0;\infty)$.

4.4 Frictional Unilateral Contacts

For true Coulomb friction the normal reaction is not known a priori. The constraint set is no longer a Cartesian product of cylinders $\tilde{\mathcal{F}}$ but a Cartesian product of cones, whose apertures are determined by the coefficients of friction. However, replacing $\tilde{\mathcal{F}}$ in Eq. (61) has the effect that the VI then, in the case of a dynamic contact,

allows solutions, which have a displacement in normal direction since the normal cone on the boundary of a cone does not reside in the tangential plane but has a normal component too. Even though this does not capture the precise frictional behaviour one can physically interpret these vertical motions as surface asperities [1].

As in the case of pseudo-friction we now can describe the time step problem as a VI

$$\boldsymbol{x} \in \delta t\tilde{\mathcal{C}}, \quad ((\mathbf{A}^T\mathbf{A} + s\mathbf{D})\boldsymbol{x} - \mathbf{A}^T\boldsymbol{b})^T(\boldsymbol{y} - \boldsymbol{x}) \geq 0, \quad \forall \boldsymbol{y} \in \delta t\tilde{\mathcal{C}}, \tag{64}$$

where $\tilde{\mathcal{C}}$ is $\prod_i \{\boldsymbol{x} \in \mathbb{R}^3 | x_n \geq 0, \|\boldsymbol{x}_{t,o}\|_2 \leq \tilde{\mu}_i x_n\}$ but still convex and thus as before the solution we look for is the weighted minimum norm solution

$$\|\mathbf{D}^{\frac{1}{2}}\boldsymbol{x}\|_2^2 = \min_{\boldsymbol{x} \in \delta t\tilde{\mathcal{C}}, (\mathbf{A}^T\mathbf{A}\boldsymbol{x} - \mathbf{A}^T\boldsymbol{b})^T(\boldsymbol{y}-\boldsymbol{x}) \geq 0, \ \forall \boldsymbol{y} \in \delta t\tilde{\mathcal{C}}} \boldsymbol{x}^T\mathbf{D}\boldsymbol{x}. \tag{65}$$

The situation changes for true Coulomb friction though and a rigorous analysis is yet to be done.

5 Conclusion

In this report the ill-posedness of rigid multibody problems is demonstrated by means of a table sliding down a ramp. It is argued that a reasonable regularization can be to insert springs at contacts or bilateral joints and then homogeneously increase the spring stiffnesses. These regularized systems are discretized and two conclusions are drawn: In the stiff limit a typical rigid multibody system is obtained and when increasing the spring stiffness the solution approaches a weighted minimum norm solution of the unregularized system. This was demonstrated for bilateral joints, frictionless as well as simplified frictional systems. Systems with true Coulomb friction however pose an open problem. Even though the regularization approach can be directly transformed into a numerical scheme iteratively reducing the regularization parameter a more efficient numerical scheme is to be found.

References

[1] M. Anitescu. Optimization-based simulation of nonsmooth rigid multibody dynamics. *Math. Program.*, 105(1):113–143, 2006.

[2] M. Anitescu and F.A. Potra. Formulating dynamic multi-rigid-body contact problems with friction as solvable linear complementarity problems. *ASME Nonlinear Dynamics*, 14:231–247, 1997.

[3] R.W. Cottle, J.-S. Pang, and R.E. Stone. *The Linear Complementarity Problem.* Academic Press, Inc., 1992.

[4] R.W. Cottle, J.-S. Pang, and R.E. Stone. *The Linear Complementarity Problem.* Society for Industrial and Applied Mathematics, 2009.

[5] G.M. Lee, N.N. Tam, and N.D. Yen. *Quadratic Programming and Affine Variational Inequalities: A Qualitative Study.* Springer Science+Business Media Inc., 2005.

[6] C. Popa and T. Preclik. Iterative Solution of Weighted Least Squares Problems with Applications to Rigid Multibody Dynamics. Technical report, Friedrich-Alexander University Erlangen-Nuremberg, November 2010.

[7] J. Sauer and E. Schömer. A constraint-based approach to rigid body dynamics for virtual reality applications. In *Proceedings of the ACM symposium on Virtual reality software and technology*, pages 153–162, 1998.

[8] Xiubin Xu and Hong-Kun Xu. Regularization and Iterative Methods for Monotone Variational Inequalities. *Fixed Point Theory and Applications*, 2010:11, 2010.